06

Study of characteristics of magnetic nanoparticles produced by laser ablation

© U.E Kurilova,[1,2,3] A.S. Chernikov,[2] D.A. Kochuev,[2] R.V. Chkalov,[2] M.A. Dzus,[2] A.V. Kharkova,[2] A.V. Kazak,[2,4] I.A. Suetina,[5] L.I. Russu,[5] M.V. Mezentseva,[5] K.S. Khorkov[2]

[1] World-class research center „Digital biodesign and personalized healthcare“,
I.M. Sechenov First Moscow State Medical University, Ministry of Health of the Russian Federation,
119991 Moscow, Russian Federation
[2] Institute of Information Technology and Electronics, Vladimir State University
named after Alexander Grigorievich and Nikolay Grigorievich Stoletov (VlSU),
600000 Vladimir, Russia
[3] Institute of Biomedical Systems, National Research University „MIET“,
124498 Moscow, Zelenograd, Russia
[4] Tekhnopark, State University of Education,
105005 Moscow, Russia
[5] National Research Center for Epidemiology and Microbiology named after Honorary Academician N.F. Gamaleya, Ministry of Health of the Russian Federation,
123098 Moscow, Russia
e-mail: kurilova_10@mail.ru

Received December 23, 2024
Revised December 23, 2024
Accepted December 23, 2024

The article presents the results of magnetic nanoparticles studies for biomedical applications. Nanoparticles were synthesized by laser ablation in deionized water and acetone with subsequent magnetic separation. Raman spectroscopy indicates the predominance of magnetite particles among the obtained material. Scanning electron microscopy studies indicate a spherical shape of the particles, their size is 70 nm when synthesized in deionized water and 64 nm when synthesized in acetone. The cytotoxicity of nanoparticles was studied for connective tissue cells and tumor cells using a colorimetric test for assessing cell activity and fluorescence microscopy. It was found that nanoparticles are non-toxic for healthy cells, while a decrease in the number of tumor cells is achieved at a colloidal solution concentration of nanoparticles of more than 1.7 μg/ml, the creation of nanoparticles in acetone and transfer to a non-toxic solvent does not reduce the survival of cells. The results of the study indicate the prospects for the use of synthesized nanoparticles for biomedical applications related to theranostics of socially significant diseases.

Keywords: laser ablation, iron nanoparticles, magnetic separation, theranostics, cytotoxicity.

DOI: 10.61011/TP.2025.05.61123.440-24

Introduction

Currently, metallic nanoparticles are extensively used for dealing with various theranostics problems. Iron-based magnetic nanoparticles are of great interest to the scientific community, as they are distinguished by the highest level of biocompatibility [1]. Most of their applications are the result of magnetic properties that differ significantly from those of a bulk material.

High biocompatibility, low production costs and the ability to control magnetic nanoparticles position in the biological tissue under exposure to magnetic field allows their using for targeted delivery of therapeutic agents to various areas of the body [2], including against blood flow or through impenetrable areas [3]. Magnetic nanoparticles in theranostics may be used for vascular assessment and visualization of atherosclerotic plaques [4], for targeted delivery of antibiotics or antiviral agents, as well as for the diagnosis of pathogens [5]. In case of such a common disease as osteoarthritis, nanoparticles can be functionalized by drug molecules (dexamethasone, methotrexate, etc.) and precisely delivered to the injury area, which increases the therapeutic effect due to local use, higher release and prolonged retention of drug molecules in the target area [6]. Magnetic nanoparticles also have prospects for the diagnosis of oncological diseases, where early diagnosis and complete destruction of tumor cells with maximum preservation of healthy tissue are of the greatest importance [1]. When irradiated with laser radiation or an alternating magnetic field, magnetic nanoparticles can heat up, thereby destroying tumor tissues. It is possible to increase the effectiveness of therapy by adding molecules activated by temperature increase to magnetic nanoparticles [7]. In addition, magnetic nanoparticles may act as contrast agents during diagnostics via magnetic-resonance imaging, selectively accumulating in tumor tissues due to various active and passive targeting techniques. In this case, by increasing the rate of proton relaxation, the image contrast increases and the required

dose of nanoparticles decreases, which is an important advantage over existing contrast agents that have side effects [8]. Further heating of such particles makes it possible to effectively combine the diagnosis and removal of tumors in one procedure [9]. Additionally, it is possible to change the necessary parameters of magnetic nanoparticles by creating a polymer shell around them. The presence of the shell may affect the processes of interaction of nanoparticles with living cells, the pattern of their distribution in the volume of biological tissue and excretion from the body [10].

Such characteristics of nanoparticles as their size, shape, surface charge, degree of aggregation, surface morphology, and others have a direct impact on their behavior in a living organism. These parameters shall be taken into account when evaluating the interaction of nanoparticles with cells and tissues, which may affect their biological activity and therapeutic potential.

The size of nanoparticles is one of the key parameters that determine the mechanics of nanoparticle passage through body systems. Smaller nanoparticles can effectively penetrate the cell membranes and interact with cellular structures. At the same time, large particles can be trapped in the organs of the body's immune system [11]. The shape of the nanoparticles also matters. Studies show that spherical nanoparticles may have different mechanisms of interaction with cells compared to elongated or heterogeneous ones. This can affect their distribution in the body and the rate of elimination from the body, for example, nanoparticles with a high aspect ratio tend to stay in tissues for longer periods of time [12].

The surface charge of nanoparticles affects their interaction with cells and other molecules in biological systems. Charged surfaces can contribute to formation of layers of the solvent molecules, which changes stability of suspensions and may affect the adsorption of proteins and other biomolecules. This, in its turn, may change the immune response of the body for release of the nanoparticles [11]. Particles stability and tendency to aggregation are also important parameters in determining the behavior of nanoparticles in the body. Aggregation may lead to formation of larger structures featuring different physicochemical properties and behavior compared to individual particles, which affects their distribution in the body and their ability to reach the target tissues [13]. The morphology of the nanoparticle surface is another important aspect that needs to be taken into account. Irregularities and roughness, as well as surface composition, can affect the adhesion of particles to the cell membranes and their interaction with plasma proteins [14].

There are several methods for the synthesis of magnetic nanoparticles, such as chemical deposition from the gas phase, thermal decomposition, micro-emulsion method, laser ablation, etc. [15]. The choice of the synthesis method is determined by the required characteristics of nanoparticles: their size, surface charge, necessary state of the dispersed medium, stability, purity, etc. The laser ablation method is promising, as it allows flexible control of physical processes under laser exposure and the use of additional sources of external influence to regulate the synthesis process. Within the framework of this method, it is possible to synthesize nanoparticles in both liquids and gases. Its key benefits are the absence of toxic chemicals used in the synthesis process, high efficiency, and ability to produce nanoparticles with high saturation magnetization. The resulting nanoparticles have high frequency, suitable for use in a body. In case of fabrication of magnetic nanoparticles, it is possible to carry out magnetic separation by selecting particles with magnetic properties with the help of external magnetic field [16].

Thus, each new type of synthesized nanoparticles shall be carefully characterized in terms of physical characteristics and biocompatibility with living cells. Careful delineation of characteristics will help to evaluate the nanoparticles behavior in the body and will allow the development of more effective and safe nanomaterials for medical and biological applications.

In the present paper, magnetic nanoparticles were synthesized by laser ablation in a liquid medium and then subjected to magnetic separation for collection of nanoparticles. The morphological characteristics of the obtained nanoparticles were analyzed based on the results of scanning electron microscopy, and the composition of the nanoparticles was analyzed using Raman scattering spectroscopy. The biocompatibility of nanoparticles *in vitro* was investigated on two cell lines: connective tissue cells (fibroblasts) and tumor cells (neuroblastoma).

1. Materials and research methods

1.1. Synthesis of nanoparticles

Colloidal solutions of nanoparticles obtained by laser ablation in a liquid medium were used for the research.

Sample 1 — nanoparticles obtained in the deionized water from which the magnetic particles were taken. The nanoparticle suspension was a black solution with a concentration of nanoparticles of 0.45mg/ml.

Sample 2 — nanoparticles obtained in acetone from which the magnetic particles were taken and placed to the deionized water. The nanoparticle suspension was a black solution with a concentration of nanoparticles of 1 mg/ml.

The synthesis of nanoparticles by laser ablation in liquid was carried out using the developed laser ablation and fragmentation of nanoparticles [17]. The target was processed using a laser source that generated pulses with a duration of 280 fs with a maximum energy of up to 150 μJ and a wavelength of 1030 nm. The target, which is a tablet made of pure iron, was placed in a quartz cuvette. The nanoparticles were ablated at laser radiation energy of 50 μJ. The laser beam moved evenly over the surface of the target using a scanning system, thanks to which the laser could continuously process various parts of the target, creating homogeneous impact zones.

Laser radiation passed through a special window in the upper part of the synthesis unit. Position of the treated sample and the process of laser ablation of nanoparticles and their movement in a magnetic field were recorded using a CCD camera through an inspection window. The target was ablated for 900 s in deionized water and 1500 s when using acetone as a solvent.

In the experiments the separation of nanoparticles was carried out using a permanent magnet with a maximum magnetic field of 0.5 T, on which a tube with a colloidal solution was installed. The obtained nanoparticles in the state of colloidal solutions were subjected to magnetic separation under the action of magnetic induction for 600–900 s, while nanoparticles with a magnetic moment precipitated from the solution onto the cuvette wall, after which the liquid medium was removed several times and replaced with a clean one. Before conducting all further studies, colloidal solutions of nanoparticles were treated with ultrasound.

1.2. Scanning electron microscopy

The morphology of synthesized nano-materials was studied with the use of a scanning electron microscope (SEM) Quanta 200 3D (FEI). To prepare the samples the volume of 10 μl of colloidal solution was deposited on the surface of a pre-cleaned silicon wafer, which was located on a magnet, and then dried at room temperature. The samples were attached to the holder by means of a carbon ribbon. The accelerating voltage of the electronic beam was 30 kV, electronic probe current - 91 pA. The analysis of SEM images to estimate the particle size distribution was carried out manually in ImageJ software.

1.3. Raman scattering spectroscopy

The Raman scattering spectra of the samples were measured using the probe nanolab NTEGRA Spectra (NT-MDT). The excitation source in measurements was a laser with a wavelength of 473 nm, the measurements were carried out using a diffraction grating 1800 lines/mm. The samples were prepared for the study in the same way as preparation for the scanning electron microscopy.

1.4. Cell culture for tests *in vitro*

The study was conducted using two types of cells: FECH (fibroblasts cell line of a human embryo) — a cell line of human connective tissue, Neuro 2A — a cell line of mouse glioblastoma. The fibroblast cell line was produced from a collection of cell cultures by the Gamaleya National Center of Epidemiology and Microbiology. For the preliminary cell growth, a medium modified by the Dulbecco method was used — 90% cell culture solution, with 10% calf serum. When the required amount was reached, the cells were removed from the bottom of the culture vial, the resulting cell suspension was poured into sterile tubes and then used for experiments. To determine the seed dose, an automatic cell counter Scepter Millipore was used, which was calculated immediately before the experiments.

1.5. Studies of cytotoxicity of the nanoparticles via MTT assay

FECH cell seed dose was $3.8 \cdot 10^5$ cells/ml, Neuro 2A cells— $2.5 \cdot 10^5$ cells/ml. To conduct the study, cells in the amount of 200 μl were placed in the wells of a 96-well plate and cultured in a CO_2 thermostat for 24 h. Next, 200 μl of the nanoparticle solution was placed in the first column of the tablet and mixed with cells using a dispenser, then 200 μl of the nanoparticle solution with cells were placed in the second column of the tablet and mixed with a dispenser, etc. Thus, the concentration of nanoparticles in each column of the tablet decreased by 2 times. After 48 hours of cells cultivation with nanoparticle solutions, an MTT assay was performed according to the standard procedure described by T. Mosmann [18]. MTT was added to each well (3-(4.5-dimethylthiazol-2-yl)-2.5-diphenyl-tetrazolium bromide), which was in the wells for 2 hours, then dimethyl sulfoxide was added and the numerical value of the optical density at a wavelength of 545 nm was detected using flatbed photocolorimeter Immunochem-2100. The comparison was performed relative to the control value obtained for wells of a tablet with a cell suspension without adding any samples, which were calibrated in a similar way.

1.6. Fluorescence microscopy of cells

Apart from the MTT-assay, the cells of FECH were studied through microscope in the presence of several concentrations of nanoparticles: for a sample of magnetic nano-particles obtained in water the dilutions of 1 to 100 were studied (final concentration — 4.5 μg/ml) and 1 to 500 (final concentration — 0.9 μg/ml), for a sample of magnetic nano-particles obtained in acetone — dilution of 1 to 500 (final concentration — 10 μg/ml). The experiment was carried out as follows: sterile cover glasses were placed on the bottom of the wells of the culture plate. Next, 2 ml cells were added to the wells, and the tablet was placed in a thermostat. After 24hours, nanoparticles were added to the solution to achieve the required dilution: 20 μl for dilution 1 to 100 and 4 μl for dilution 1 to 500. The samples with nanoparticles were further kept in a thermostat for 48 h, after which they were stained with Hoechst 33342 dye and observed with fluorescence microscope an Olympus BX43.

2. Results and discussion

2.1. Features of morphology, size, and chemical composition of nanoparticles

Fig.1 shows SEM images of nanoparticles obtained as a result of femtosecond laser ablation of iron in deionized water (Fig. 1, *a*) and in acetone (Fig. 1, *b*) selected by

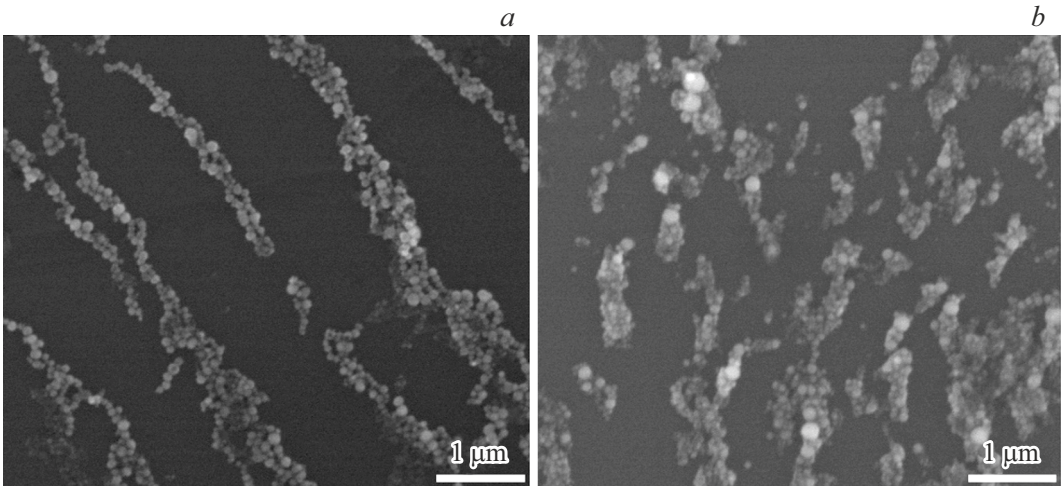

Figure 1. SEM images of nanoparticles obtained as a result of femtosecond laser ablation of iron in deionized water (*a*) and in acetone (*b*) selected by magnetic separation.

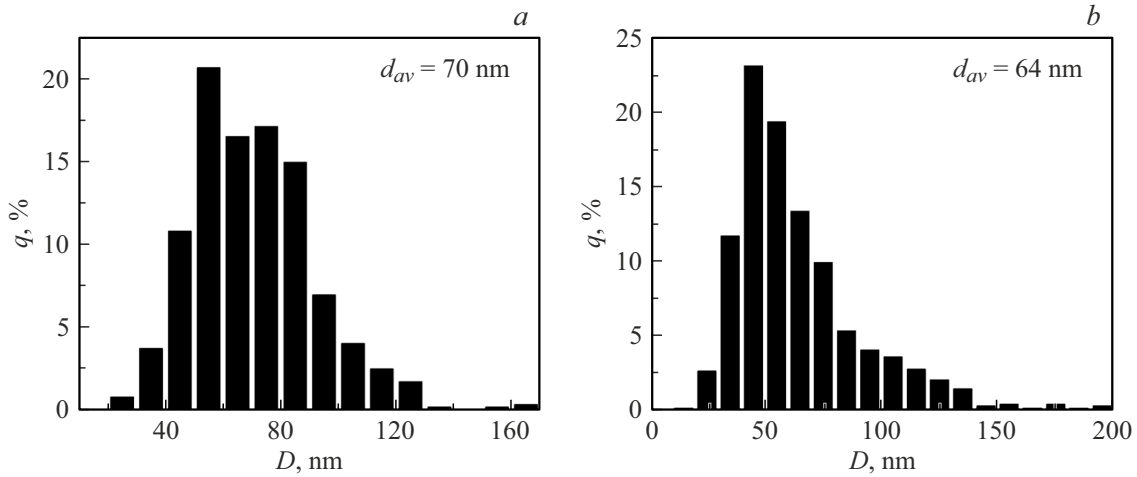

Figure 2. Histograms of size distribution of magnetic nanoparticles obtained as a result of femtosecond laser ablation of iron in deionized water (*a*) and in acetone (*b*).

magnetic separation. Fig.2 also shows the histograms of size distribution of magnetic nanoparticles obtained as a result of femtosecond laser ablation in deionized water (Fig. 2, *a*) and in acetone (Fig. 2, *b*). Individual nanoparticles are 20–100 nm in size, the nanoparticles are spherical in shape. The nanoparticles are agglomerated in parallel lines along the direction of the magnetic field. This effect is observed more clearly for nanoparticles obtained by laser ablation in an aqueous medium, which is clear for understanding, since acetone evaporates much faster and the time for arranging nanoparticles under the influence of a magnetic field is very limited.

The average size of nanoparticles obtained by laser ablation in deionized water selected by magnetic separation is 70 nm, and in the case of magnetic nanoparticles synthesized in acetone 64 nm. During synthesis in water, a smaller size spread of nanoparticles is observed, most of them are in the range of 50–90 nm.

According to literature data, the optimal size of magnetic nanoparticles for biological applications lies in the range of 10–200 nm, in which case the nanoparticles remain in the body for a sufficient amount of time to achieve a therapeutic effect. At the same time, large magnetic nanoparticles have a more pronounced cytotoxic effect in alternating low-frequency magnetic fields compared with smaller ones [19].

Figure 3 shows the Raman scattering spectrum of nanoparticles synthesized by laser ablation of iron in deionized water, selected by magnetic separation.

Availability of peaks at 305, 539 and 560 cm^{-1}, corresponding to modes E_g, T_{2g} and A_{2g} of magnetite proves primarily the presence of Fe_3O_4, the peak is observed at 357 cm^{-1}, which may be attributed to mode T_1 γ-Fe_2O_3. (maghemite).

To measure Raman scattering spectra of nanomaterials obtained as a result of laser ablation in acetone (Fig. 4), particles were transferred from the initial medium (acetone)

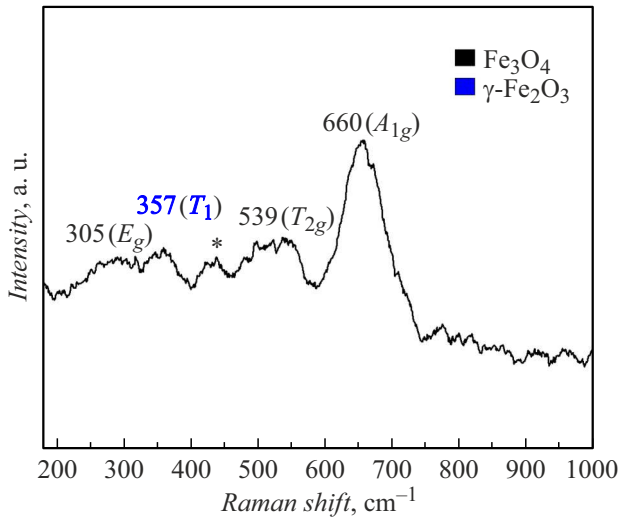

Figure 3. Raman scattering spectrum of nanoparticles synthesized by laser ablation of iron in deionized water, selected by magnetic separation.

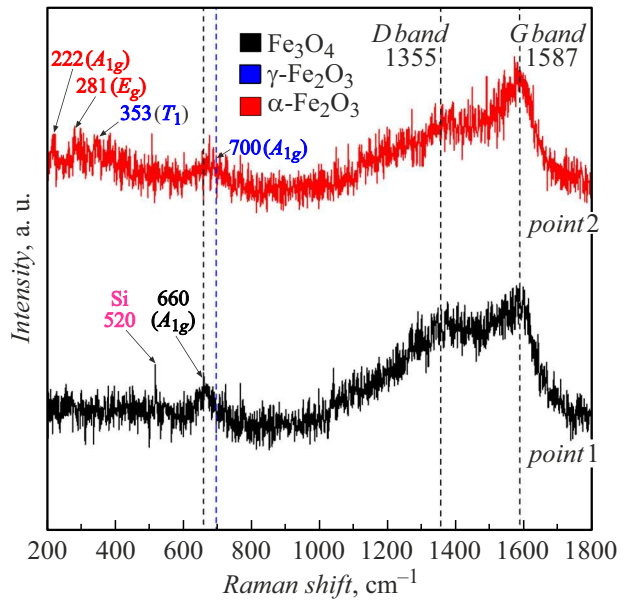

Figure 4. Raman scattering spectra of nanoparticles synthesized by laser ablation of iron in acetone, selected by magnetic separation, taken at two points of the sample (designated point 1, point 2).

to deionized water. The measurements were carried out at two different points of the sample deposited on the silicon surface.

Raman scattering spectra contain the carbon-associated carbon peaks at 1355 cm^{-1} (*D*-band of a crystalline structure) and 1587 cm^{-1} (*G*-band relating to the oscillations in the coupling plane C–C) [20,21]. The presence of carbon phase can be explained by the decomposition of solvent molecules during laser ablation, and the formation of particles encapsulated in a carbon shell can be assumed [22].

When measuring at different points a peak is observed at 660 cm^{-1} corresponding to A_{1g} mode of magnetite; additionally, the broadening of peak may be observed in this region with an extra peak at 700 cm^{-1} and peak at 353 cm^{-1}, that may be attributed to mode A_{1g} and T_1 of maghemite, also peaks are observed at 222 and 281 cm^{-1} (modes A_{1g} and E_g α-Fe_2O_3 (hematite)). According to literature data, maghemite peaks are found in the region of about 350, 500 and 700 cm^{-1}, as well as a peak in the high-frequency region of about 1400 cm^{-1} [23,24], the recorded range fully includes the expected peaks from magnetic nanoparticles. Unlike hematite and magnetite, the Raman scattering bands of maghemite are indistinctly defined, and their position depends on the sample manufacturing method, which affects the degree of crystallinity. As the size of the nanoparticles decreases, scattering decreases and some of the peaks may disappear [25]. Thus, the absence of other peaks of maghemite in the spectrum, except the peak 357 cm^{-1} and a wide peak in the region 660–700 cm^{-1}, is explained by a combination of features of nanoparticles fabrication method and their relatively small size. We also cannot exclude that the peaks may be overlapped in the region 1350–1400 cm^{-1}, here, we mean *D*-band and peak of about 1400 cm^{-1} specific for maghemite. However, the intensity of this peak is significantly lower than the intensity of the peak corresponding to *D* band. In addition, when the energy of the exciting laser increases, oxidation to hematite occurs, peaks characteristic of magnetite and maghemite are not observed, while peaks at 1355 and 1387 cm^{-1} remain, which may serve as an indirect confirmation of the carbon shell presence. When using maximum energy, there are no bands in the Raman scattering spectra *D*- and *G*-, and only peaks characteristic of hematite are observed. The observed changes in the Raman scattering spectra with increasing energy of the exciting laser indicate the destruction of the carbon shell and the dominance of signals from the oxidized surface of nanoparticles.

The most suitable metal oxide nanoparticles for biomedical applications are Fe_3O_4, γ-Fe_2O_3 and spinel ferrites due to their biocompatibility, high oxidative stability, high magnetic moments, low toxicity and high chemical stability under physiological conditions [11].

2.2. MTT assay

According to the experimental data, graphs of the dependences of cytotoxicity of nanoparticle solutions on their concentration were obtained (Fig. 5). These graphs show a decrease in the cytotoxic properties of synthesized nanoparticles as their concentration decreases. For dilutions of 1 to 2, 1 to 4, and 1 to 8, some distortions of the results were observed in one or more repeated experiments. This is due to the fact that at high concentrations of nanoparticles, they aggregated and settled on the bottom of the well, as a result of which they could not be removed from the there and made an error in the final result.

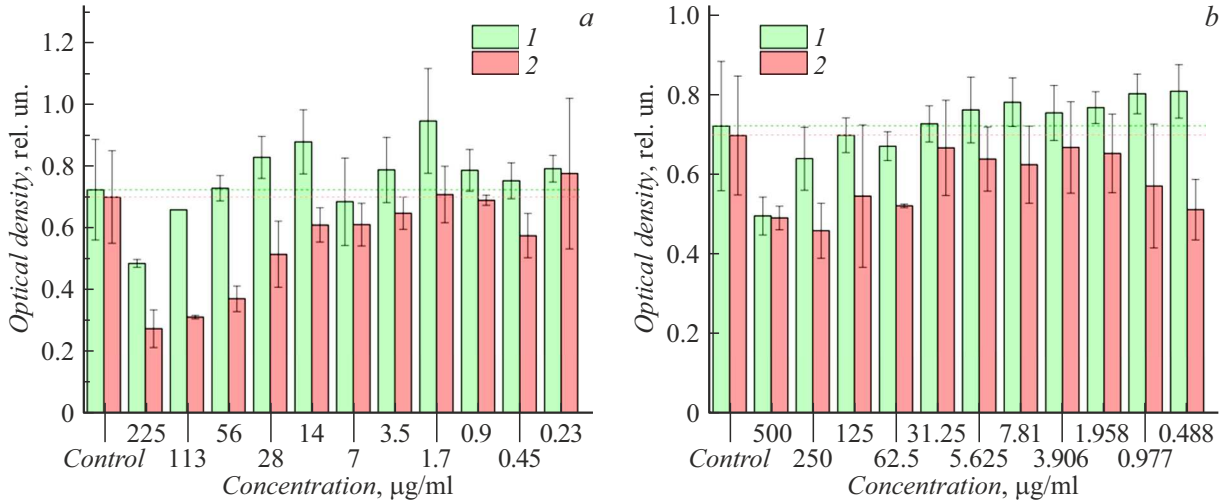

Figure 5. Comparative curves of cytotoxicity dependence of colloidal solutions of nanoparticles obtained by laser ablation in water (*a*) and in acetone (*b*) for different cell types: FECH (*1*) and Neuro 2A (*2*). Levels of control were shown by dashed lines.

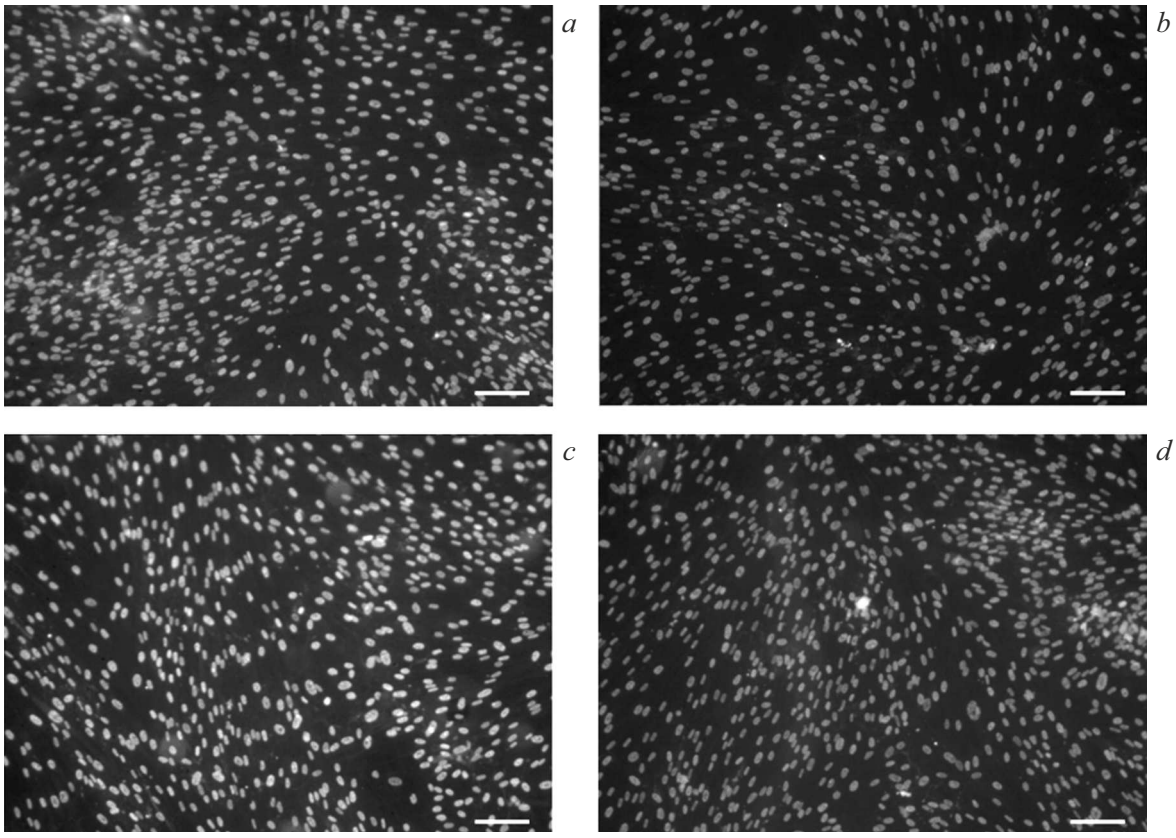

Figure 6. Micro-photos of cells in colloidal solutions of nanoparticles: *a* — sample 1, diluted as 1 to 100; *b* — sample 1, diluted as 1 to 500; *c* — sample 2 diluted as 1 to 500; *d* — control. Scale line — 100 μm.

According to the graphs, it can be concluded that nanoparticles do not have toxic effects on healthy cells at concentrations below 56 μg/μl in case of magnetic nanoparticles synthesized in deionized water and below 125 μg/ml in case of a sample of nanoparticles synthesized in acetone and transferred further into deionized water. At the same time, these concentrations inhibit the growth of tumor cells. In a sample of particles synthesized in acetone, the survival rate of tumor cells does not exceed the control level with any dilution of nanoparticles, which indicates the possibility of using synthesized nanoparticles to inhibit tumors. For the nanoparticles in aqueous solution such effect was observed when the concentration of nanoparticles was higher than 1.7 μg/ml.

Various papers devoted to the synthesis of magnetic nanoparticles indicate their low toxicity to the human body along with the preservation of magnetic properties. The studies, where toxicity of nanoparticles of various metal oxides (CuO, TiO_2, ZnO, $CuZnFe_2O_4$, Fe_3O_4 and Fe_2O_3) *in vitro* were compared, revealed that iron oxides were not toxic or had very low toxicity in concentrations of $20-100\,\mu$g/ml. Other studies *in vitro*, depending on the type of studied cells and the presence of a shell for iron oxide nanoparticles (surfactant or polymer), showed that the limit of toxicity of iron nanoparticles lies in the concentration range from 10 to $1000\,\mu$g/ml [26]. The concentration obtained in this work is also in these ranges, and the toxicity can additionally be reduced by forming a shell on the surface of the particles.

2.3. Microscopy of cells on magnetic nanoparticle samples

The obtained microscopic images are shown in Figure 6. The size and morphology of the cells in the experimental samples do not differ from the reference ones. The cells have an elongated fusiform shape, which is inherent in normally functioning cells after more than 3 hours of cultivation on the surface, the nuclei are colored much more intensively than the cytoplasm due to the peculiarities of the dye accumulation. The cell sizes reach $100-150\,\mu$m, the size of the cell nuclei is about $20\,\mu$m. After 48 h of cells cultivation with samples of magnetic nanoparticles, the formation of a monolayer and almost complete cell coverage on the slide cover are revealed. The number of cells in the experimental samples is not reduced compared to the control, their uniform distribution over the surface is observed.

Thus, the studies *in vitro* have shown that the considered solutions of magnetic nanoparticles are safe for healthy cells. At the same time, there are a number of concentrations that have an oppressive effect on tumor cells, which is promising for the use of synthesized magnetic nanoparticles in the treatment of oncological diseases. Safety of nanoparticle concentrations in the range from 1.7 to $56\,\mu$g/μl for a sample of magnetic nanoparticles obtained in an aqueous medium and concentrations from 31.25 to $56\,\mu$g/μl for a sample of magnetic nanoparticles obtained in acetone is a key aspect that can significantly improve the effectiveness of treatment while minimizing possible side effects.

The use of nanoparticles in these limited concentrations is possible as a targeted transport of therapeutic molecules. Using this method helps to reduce the systemic side effects associated with traditional methods of chemotherapy, since the active substances will be released exactly in those areas where they are most needed. This is achieved by moving the nanoparticles with a magnetic field to the desired area, where the nanoparticles are able to accumulate resulting in a high concentration of the active substance. External magnetic field can also be used to hold nanoparticles within a given area, which is extremely important, for example, for the treatment of osteoarthritis, or for the complete destruction of tumor cells using hyperthermia, which is another promising treatment method. The nanoparticles in this method serve as heaters that convert the applied oscillatory magnetic field into thermal energy (range $41-47\,^\circ$C). Such an increase in temperature can cause thermal destruction of tumor cells or make them more susceptible to the effects of other therapeutic agents. The nanoparticles are injected as a colloidal suspension and selectively accumulate in the tumor area. Accumulation can occur either passively due to the altered structure of the vessels feeding the tumor, or actively through the use of specific surface ligands. The effect of magnetic nanoparticles on tumor cells can be controlled externally by adjusting the applied magnetic field. The applied electromagnetic radiation lies in the safe radio frequency band (from several kHz to 1 MHz), while penetrating deeply into internal organs and tissues. It was found that tumor cells have a higher sensitivity at the temperatures above $42\,^\circ$C; at this temperature the cells demonstrate no enzymatic activity [28].

Thus, the considered dilutions are safe for healthy cells, which, along with the inhibitory effect on tumor cells, indicates the possibility of using synthesized magnetic nanoparticles for the treatment of oncological diseases with minimizing side effects. It can also be concluded that the obtained magnetite nanoparticles are safe both during direct synthesis in deionized water and during synthesis in acetone and subsequent transfer to a non-toxic solvent.

Conclusion

In this paper, aspects of synthesis of nanoparticles with magnetic properties in two solvents are considered: in distilled water and in acetone (with subsequent transfer to distilled water). The nanoparticles were synthesized by laser ablation in a liquid and subjected to separation to isolate and select the magnetic particles. The obtained nanoparticles were characterized for both synthesis variants, the majority of nanoparticles have a spherical shape and sizes up to 100 nm, the average sizes are 70 nm when synthesized in deionized water and 64 nm when synthesized in acetone. Cytotoxicity studies indicate a low level of toxic effect of particles on living cells at concentrations below $56\,\mu$g/μl for a sample of nanoparticles obtained in aqueous medium, and below $125\,\mu$g/ml for nanoparticles obtained in acetone and placed in water. At the same time, lower concentrations of nanoparticles are necessary for the death of tumor cells, which indicates that it is possible to select a safe and effective concentration of nanoparticles in theranostics of oncological diseases. Thus, the synthesized magnetic nanoparticles have high potential for clinical use and may become the basis for creation of new therapeutic approaches within the framework of innovative methods of treating socially significant diseases, contributing to more effective treatment with minimal risks for patients.

Funding

The study of processes of formation and characterization of nanoparticles was supported by the Russian Science Foundation (grant No. 22-79-10348). The studies on investigation of nanoparticles biocompatibility were supported by the Ministry of Education and Science of the Russian Federation (project FSMR-2024-0003).

Conflict of interest

The authors declare that they have no conflict of interest.

References

[1] O.L. Gobbo, K. Sjaastad, M.W. Radomski, Y. Volkov, A. Prina-Mello. Theranostics, **5** (11), 1249 (2015). DOI: 10.7150/thno.11544
[2] X. Li, W. Li, M. Wang, Z. Liao. J. Controlled Release, **335**, 437 (2021). DOI: 10.1016/j.jconrel.2021.05.042
[3] A. Coene, J. Leliaert. J. Appl. Phys., **131**, 16 (2022). DOI: 10.1063/5.0085202
[4] K.X. Vazquez-Prada, J. Lam, D. Kamato, Z.P. Xu, P.J. Little, H.T. Ta. Arteriosclerosis, Thrombosis, and Vascular Biology, **41** (2), 601 (2021). DOI: 10.1161/ATVBAHA.120.315404
[5] S.K. Jat, H.A. Gandhi, J. Bhattacharya, M.K. Sharma. Mater. Adv., **2** (14), 4479 (2021). DOI: 10.1039/D1MA00240F
[6] J. Li, H. Zhang, Y. Han, Y. Hu, Z. Geng, J. Su. Theranostics, **13** (3), 931 (2023). DOI: 10.7150/thno.78639
[7] R. Afzalipour, S. Khoei, S. Khoee, S. Shirvalilou, N.J. Raoufi, M. Motevalian, M.Y. Karimi. Nanomedicine: Nanotechnology, Biology and Medicine, **31**, 102319 (2021). DOI: 10.1016/j.nano.2020.102319
[8] L. Zhu, Z. Zhou, H. Mao, L. Yang. Nanomedicine, **12** (1), 73 (2017). DOI: 10.2217/nnm-2016-0316
[9] K. Hayashi, M. Nakamura, W. Sakamoto, T. Yogo, H. Miki, S. Ozaki, K. Ishimura. Theranostics, **3** (6), 366 (2013). DOI: 10.7150/thno.5860
[10] Z. Hedayatnasab, A. Dabbagh, F. Abnisa, W.M.A.W. Daud. Europ. Polymer J., **133**, 109789 (2020). DOI: 10.1016/j.eurpolymj.2020.109789
[11] N. Senthilkumar, P.K. Sharma, N. Sood, N. Bhalla. Coordination Chem. Rev., **445**, 214082 (2021). DOI: 10.1016/j.ccr.2021.214082
[12] A. Zhang, K. Meng, Y. Liu, Y. Pan, W. Qu, D. Chen, S. Xie. Adv. Colloid Interface Sci., **284**, 10226 (2020). DOI: 10.1016/j.cis.2020.102261
[13] J. Nowak-Jary, B. Machnicka. Intern. J. Nanomedicine, 4067 (2023). DOI: 10.2147/IJN.S415063
[14] G. Stepien, M. Moros, M. Pérez-Hernández, M. Monge, L. Gutiérrez, R.M. Fratila, J.M. de la Fuente. ACS Appl. Mater. Interfaces, **10** (5), 4548 (2018). DOI: 10.1021/acsami.7b18648
[15] S. Majidi, F. Zeinali Sehrig, S.M. Farkhani, M. Soleymani Goloujeh, A. Akbarzadeh. Artificial Cells, Nanomedicine, and Biotechnology, **44** (2), 722 (2016). DOI: 10.3109/21691401.2014.982802
[16] D.A. Kochuev, A.S. Chernikov, U.E. Kurilova,A.A. Voznesenskaya, A.F. Galkin, D.V. Abramov, A.V. Kazak, A.Yu. Gerasimenko, K.S. Khorkov. Pis'ma v ZhTF, **50** (12), 28 (2024) (in Russian). DOI: 10.61011/PJTF.2024.12.58061.19858
[17] U.E. Kurilova, A.S. Chernikov, D.A. Kochuev, L.S. Volkova, A.A. Voznesenskaya, R.V. Chkalov, K.S. Khorkov. J. Biomed. Photon. Eng., **9** (2), 020301 (2023). DOI: 10.18287/JBPE23.09.020301
[18] T. Mosmann. J. Immunolog. Methods, **65** (1–2), 55 (1983). DOI: 10.1016/0022-1759(83)90303-4
[19] E.M. Materón, C.M. Miyazaki, O. Carr, N. Joshi, P.H. Picciani, C.J. Dalmaschio, F.M. Shimizu. Appl. Surf. Sci. Adv., **6**, 100163 (2021). DOI: 10.1016/j.apsadv.2021.100163
[20] L. Bokobza, J.L. Bruneel, M. Couzi. Chem. Phys. Lett., **590**, 153 (2013). DOI: 10.1016/j.cplett.2013.10.071
[21] A.C. Ferrari, J. Robertson. Phys. Rev. B, **61** (20), 14095 (2000). DOI: 10.1103/PhysRevB.61.14095
[22] V. Amendola, P. Riello, M. Meneghetti. J. Phys. Chem. C, **115** (12), 5140 (2011). DOI: 10.1021/jp109371m
[23] M.A.G. Soler, G.B. Alcantara, F.Q. Soares, W.R. Viali, P.P.C. Sartoratto, J.R.L. Fernandez, P.C. Morais. Surf. Sci., **601** (18), 3921 (2007). DOI: 10.1016/j.susc.2007.04.029
[24] I. Chourpa, L. Douziech-Eyrolles, L. Ngaboni-Okassa, J.F. Fouquenet, S. Cohen-Jonathan, M. Soucé, P. Dubois. Analyst, **130** (10), 1395 (2005). DOI: 10.1039/B419004A
[25] A.M. Jubb, H.C. Allen. ACS Appl. Mater. Interfaces, **2** (10), 2804 (2010). DOI: 10.1021/am1004943
[26] T.I. Shabatina, O.I. Vernaya, V.P. Shabatin, M.Y. Melnikov. Magnetochemistry, **6** (3), 30 (2020). DOI: 10.3390/magnetochemistry6030030
[27] H. Aslam, S. Shukrullah, M.Y. Naz, H. Fatima, H. Hussain, S. Ullah, M.A. Assiri. J. Drug Delivery Sci. Technol., **67**, 102946 (2022). DOI: 10.1016/j.jddst.2021.102946
[28] O.A. Aladesuyi, O.S. Oluwafemi. Nano-Structures & Nano-Objects, **36**, 101053 (2023). DOI: 10.1016/j.nanoso.2023.101053

Translated by T.Zorina